



Contents lists available at ScienceDirect



Catalysis Today

journal homepage: www.elsevier.com/locate/cattod

Functionalized zeolitic imidazolate framework F-ZIF-90 as efficient catalyst for the cycloaddition of carbon dioxide to allyl glycidyl ether

Tharun Jose, Yesul Hwang, Dong-Woo Kim, Moon-II Kim, Dae-Won Park*

Division of Chemical and Biomolecular Engineering, Pusan National University, Gumjeong-gu, Busan 609-735, Republic of Korea

ARTICLE INFO

Article history:

Received 16 November 2013

Received in revised form 26 March 2014

Accepted 20 May 2014

Available online xxx

Keywords:

F-ZIF-90

Post-functionalization

Cycloaddition

Carbon dioxide

Epoxide

ABSTRACT

In this study, zeolitic imidazolate framework (ZIF-90) was synthesized from $Zn(NO_3)_2 \cdot 4H_2O$ and imidazolate-2-carboxyaldehyde (ICA), then it was post-functionalized to form F-ZIF-90 using hydrazine followed by quaternization. The ZIFs were characterized by elemental analysis (EA), BET, XRD, ^{13}C NMR, FT-IR, and SEM. The surface area and pore volume of F-ZIF-90 were smaller than those of ZIF-90 due to functionalization inside the pores. The F-ZIF-90 showed excellent catalytic activity for the synthesis of the cyclic carbonate from allyl glycidyl ether (AGE) and carbon dioxide. The effects of the reaction parameters such as catalyst amount, reaction time, CO_2 pressure, and reaction temperature on the reactivity of F-ZIF-90 were also studied, and reaction mechanism including the role of F-ZIF-90 catalyst was proposed. The F-ZIF-90 catalyst, however, partially lost its crystalline structure and superior catalytic performance when it was reused.

© 2014 Elsevier B.V. All rights reserved.

1. Introduction

Carbon dioxide, although abundant, non-toxic, cheap and non-flammable, poses challenges in its serving as an attractive C1 feedstock owing to its inertness toward many of the chemicals. By envisaging an efficient catalyst and reactive substrate, CO_2 could be successfully transformed into useful chemicals [1–5]. The reactions of carbon dioxide with oxiranes leading to the formation of five-membered cyclic carbonates are well-known examples of the chemical fixation of carbon dioxide [6–9], since the cyclic carbonates can be used for various purposes, such as for aprotic polar solvents, electrolytes for batteries, and starting materials for reactive polymer synthesis [6]. Among the various catalysts used for the synthesis of cyclic carbonates from carbon dioxide and epoxides [10–16], however, homogeneous catalyst systems suffer from problems such as separation of catalysts, low cost effectiveness of the catalyst synthesis process, and low reusability of the catalyst. Compared with homogeneous catalysts, heterogeneous catalysts could be easily separated and reused, but these catalysts have the following disadvantages: low catalytic activity and/or selectivity, low stability, and high-pressure requirement. Therefore, the development of a highly efficient solid catalyst system for the chemical

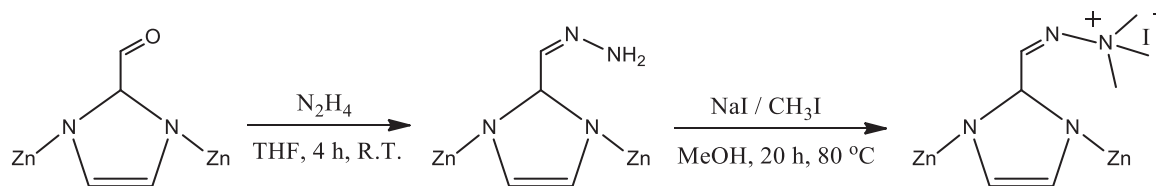
fixation of carbon dioxide under mild conditions remains a challenge.

Metal–organic frameworks (MOFs) are new emerging porous materials comprising metal centers connected by various organic linkers to create porous structures with tunable pore volumes, surface areas, and chemical properties. Enormous MOF materials have been synthesized and their numbers continue to grow rapidly, because of their zeolite-like properties, such as high internal surface area and microporosity, well-ordered porous structures and high absorption capacity [17–20]. Various applications, including gas adsorption [21], molecular separation [22], drug delivery [23], and catalysis [24,25] have been studied for the porous MOFs.

Among the reported MOFs, the subfamily of zeolitic imidazolate frameworks (ZIFs), which are based on transition metals (Zn, Co) and imidazolate linkers [26–28], have emerged as candidates for the fabrication of molecular sieve membranes and catalysts owing to their zeolite-like permanent porosity, uniform pore size, and exceptional thermal and chemical stability. Recently, Yaghi et al. [29] reported the new sodalite (SOD) topology ZIF-90 through solvothermal reaction of zinc(II) salt and imidazole-2-carboxyaldehyde (ICA). ZIF-90 is not only highly stable but also shows permanent microporosity with a narrow size of the six-membered ring pores [29]. Furthermore, the imidazole linker in ZIF-90 contains a carbonyl group, which has a favorable chemical noncovalent interaction with CO_2 . In addition, the

* Corresponding author. Tel.: +82 51 510 2399; fax: +82 51 512 8563.

E-mail address: dwpark@pusan.ac.kr (D.-W. Park).

**Scheme 1.** Post-functionalization of ZIF-90 to produce quaternized F-ZIF-90.

presence of the free aldehyde groups in the framework allows the covalent functionalization of ZIF-90 with amine group via an imine condensation reaction [29]. Recently, room-temperature synthesis [30] and water-based synthesis [31] are reported to obtain a controllable submicrometer-sized particle. Covalent post-functionalization technique was applied to prepare molecular sieve ZIF-90 membranes for enhanced hydrogen separation [32].

In this study, ZIF-90 containing free aldehyde groups in the framework was prepared and quaternized to produce functionalized F-ZIF-90, then it was used as an efficient heterogeneous catalyst for the solventless synthesis of cyclic carbonates from carbon dioxide and epoxides. It showed much higher activity than other heterogeneous catalysts reported by previous literatures.

2. Experimental

2.1. Preparation of catalyst

The synthesis of ZIF-90 was carried out with a slight modification to the synthesis procedure described by Huang et al. [33]. Imidazole-2-carboxyaldehyde (0.029 g) was slowly added to a solution of zinc nitrate tetrahydrate $[Zn(NO_3)_2 \cdot 4H_2O]$ (0.054 g) in DMF (3 mL) under stirring at room temperature for 1 h. Then the mixture was heated to 100 °C for 18 h. The precipitated solid was filtered and thoroughly washed with ethanol and dried in vacuum oven for 24 h.

The quaternary ammonium group functionalized one (F-ZIF-90) was prepared via hydrazone containing ZIF as shown in **Scheme 1**. Dried ZIF-90 crystal (1.1 mmol, 0.28 g) was reacted with hydrazine (N_2H_4 , 1 M, 10 mL) in THF at room temperature for 4 h under stirring followed by washing with THF and dried under vaccum for 24 h to form hydrazone containing ZIF, then it was mixed with CH_3OH (50 mL) and NaI (0.989 g). After adding CH_3I (0.6 mL) drop wisely, the quaternization was carried out under stirring at 80 °C for 20 h to obtain F-ZIF-90.

2.2. Characterization

FT-IR spectra of ZIF-90 and F-ZIF-90 were obtained using a Bruker A.M GMBH (960981(A)). The percentage nitrogen in the ZIFs was determined using a Vario-EL III CHN Elemental Analyzer, which used combustion in a pure oxygen environment to convert the sample elements to simple gases such as CO_2 , H_2O , and N_2 . Wide-angle X-ray diffraction (WXRD) with a Rigaku D/Max 2500 diffractometer using $Cu-K\alpha$ radiation (40 kV, 50 mA) was used to calculate d-spacing of the samples. The scanning electron microscopy (SEM) micrographs were obtained on a Hitachi S-4700 microscope operated at 30 kV. The textural properties of the samples were analyzed by recording the N_2 adsorption isotherm at 77 K, using a BET apparatus (Microneritics ASAP 2020). Before gas sorption analysis, ZIFs were pretreated for 12 h at 120 °C under vacuum. The specific surface area was determined using the BET model equation. ^{13}C cross-polarization MAS NMR spectra were measured with a recycle delay of 5 s for a total of 1024 scans with the following conditions: magic-angle spinning at 5 kHz, and a $\pi/2$ pulse of 7 μ s.

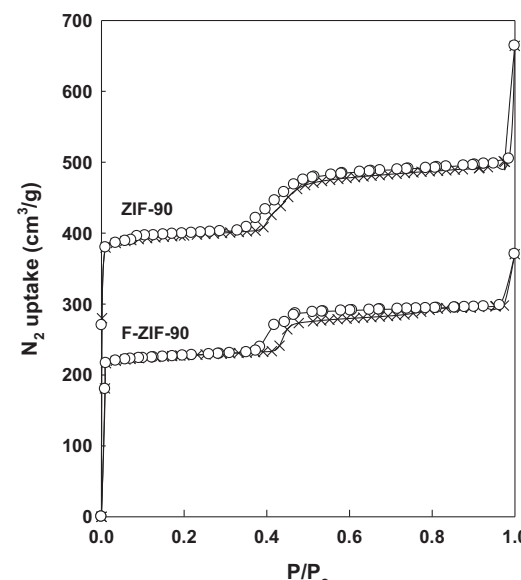
2.3. Synthesis of cyclic carbonate from AGE and CO_2

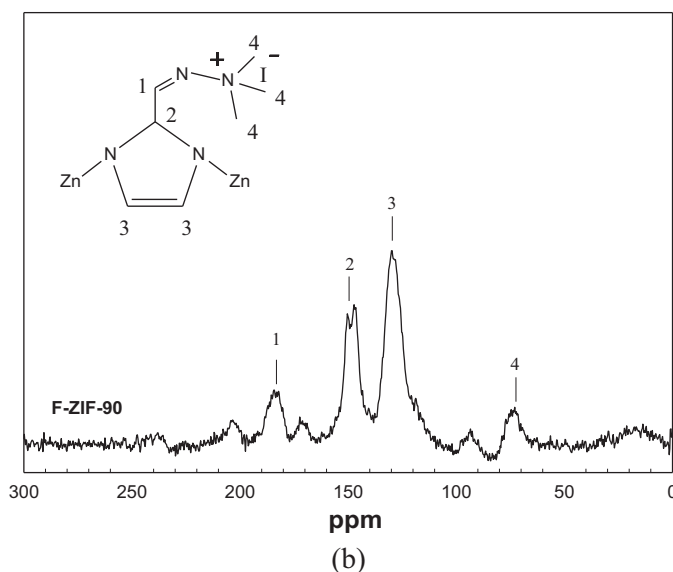
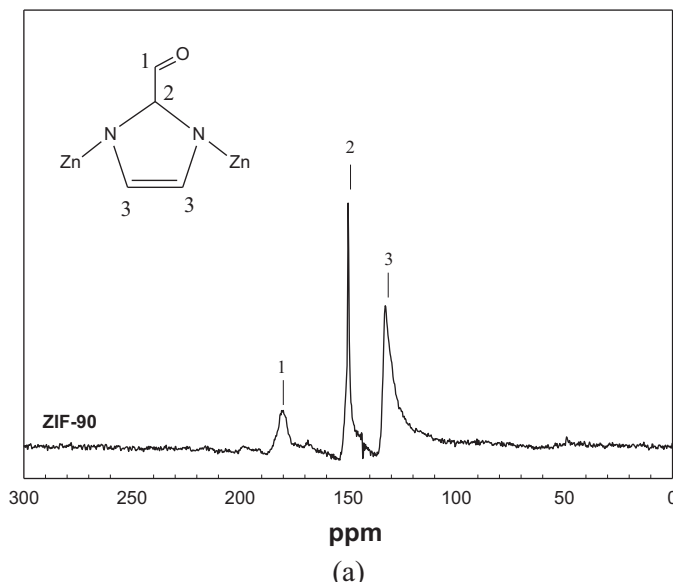
The synthesis of allyl glycidyl carbonate (AGC or 4-[(prop-2-en-1-yloxy)methyl]-1,3-dioxolan-2-one) was performed by the cycloaddition of carbon dioxide to AGE (allyl glycidyl ether or 2-[(prop-2-en-1-yloxy)methyl] oxirane). The ZIF catalyst was weighed in air and introduced into a 20-mL reactor containing 40 mmol of AGE under solvent-free conditions, and refluxed in an autoclave at a desired temperature with stirring under CO_2 atmosphere at a pressure of 0.65–1.55 MPa. In a semi-batch operation, the reactor pressure was maintained constant by a back-pressure regulator. The reactor was heated to the desired temperature, and then the reaction was started by stirring the reaction mixture at 600 rpm. After the completion of the reaction time, the cycloaddition was stopped by cooling the reaction mixture to room temperature and venting the remaining CO_2 . The product AGC was dissolved in dichloromethane and filtered to remove the catalyst. The conversion of AGE was obtained from gas chromatography (GC, HP 6890, Agilent Technologies, Santa Clara, CA, USA) data.

3. Results and discussion

3.1. Characterization of the ZIF-90 and F-ZIF-90

To perform the post-synthesis functionalization on crystals of ZIF-90 its porosity was first examined by BET analysis. The N_2 adsorption isotherm shown in **Fig. 1** indicates the permanent porosity of the ZIF-90 framework. The small step at higher relative pressure with a hysteresis loop is attributed to the formation of mesopores [34]. The presence of imine and quaternary ammonium functionalities in F-ZIF-90 severely constrict the pore aperture and

**Fig. 1.** Nitrogen isotherms of ZIF-90 and F-ZIF-90 measured at 77 K (O: desorption, X: adsorption).

Fig. 2. ^{13}C NMR spectra of (a) ZIF-90 and (b) F-ZIF-90.

prevent molecules from accessing the interior of the pores, as confirmed by its gas adsorption isotherm behavior. The BET surface area of $1328\text{ m}^2/\text{g}$ for ZIF-90 was reduced to be $763\text{ m}^2/\text{g}$ for F-ZIF-90.

To ensure aldehyde functionality of ZIF-90, the solid-state ^{13}C CP MAS NMR spectra were measured and the results are shown in Fig. 2. The ^{13}C NMR of ZIF-90 showed the resonances at 129, 150, and 178 ppm for the symmetrically equivalent 3-carbon atoms of the imidazolate, the 2-carbon atom of the imidazolate and the aldehyde carbon atom, respectively. The FT-IR spectrum of ZIF-90 is shown in Fig. 3. A strong band at 1678 cm^{-1} (C=O) provided further evidence for the presence of aldehyde in bulk ZIF-90, and the post-functionalization was confirmed by its absence in F-ZIF-90.

WXRD results for ZIF-90 and F-ZIF-90 are presented in Fig. 4. From the figure, even though the F-ZIF-90 maintained the basic crystalline structure of the parent framework (ZIF-90), its crystallinity is a little lower compared to ZIF-90 due to the quaternization process.

Table 1 also shows elemental analysis results of the ZIF-90 and F-ZIF-90. Results demonstrates the increase of nitrogen amount for

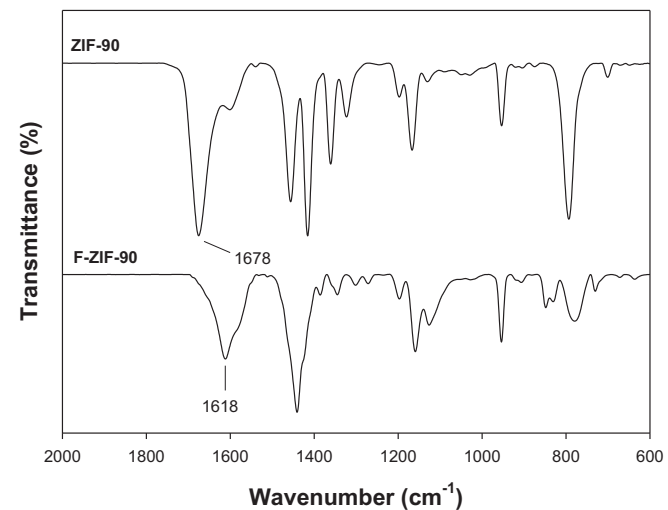


Fig. 3. FT-IR spectra of F-ZIF-90 and F-ZIF-90.

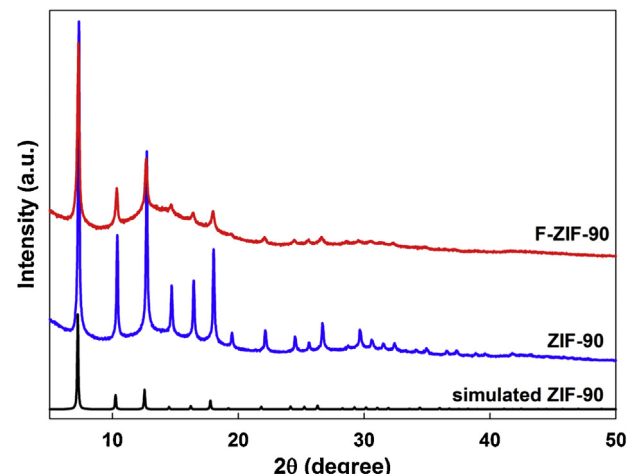


Fig. 4. WXRD patterns of ZIF-90 and F-ZIF-90.

F-ZIF-90 due to the functionalization of ZIF-90 with N_2H_4 (hydrazine) followed by the treating with alkyl halide to form it.

The morphology of F-ZIF-90 is shown in Fig. 5. In the SEM image, well-defined crystals of about $1\text{--}3\text{ }\mu\text{m}$ were observed.

3.2. Performance of ZIF-90 and F-ZIF-90

The performance of ZIF-90 and F-ZIF-90 for the synthesis of AGC was tested under batch and constant pressure semi-batch operation after a reaction time of 6 h at 120°C . The conversion of AGE, selectivity and yield of AGC are presented in Table 2. Quaternized catalyst F-ZIF-90 showed much higher AGE conversion and AGC yield than unfunctionalized ZIF-90. With only 20 mg (0.95 wt%) of F-ZIF-90 catalyst 96.6% AGC yield was obtained at constant CO_2 pressure of 1.17 MPa at 120°C . The nucleophilic nature of the iodide

Table 1
Elemental analyses of ZIF-90 and F-ZIF-90.

Catalyst	CHNO from elemental analysis			
	C (wt%)	H (wt%)	N (wt%)	O (wt%)
ZIF-90	33.86	2.47	18.59	15.32
F-ZIF-90	27.18	2.90	21.83	6.57

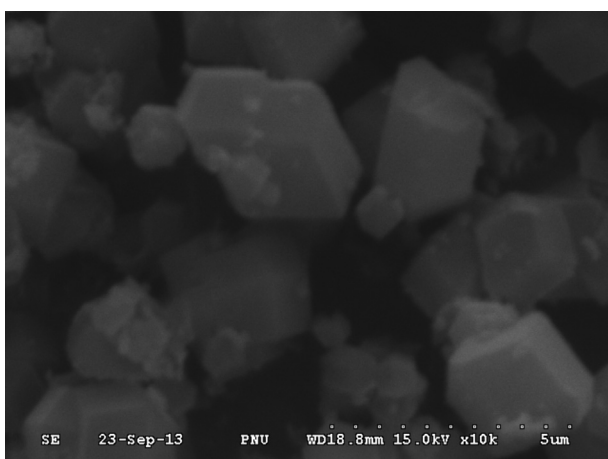


Fig. 5. SEM image of F-ZIF-90.

Table 2

The reactivity of ZIF-90 and F-ZIF-90 at batch and semi-batch operations.

Catalyst	Conv. (%)	Sel. (%)	Yield (%)
ZIF-90 ^a	64.8	61.8	40.0
F-ZIF-90 ^a	76.9	94.6	72.7
ZIF-90 ^b	86.1	50.4	43.4
F-ZIF-90 ^b	98.7	97.9	96.6

Reaction conditions: AGE = 18.1 mmol, catalyst = 20 mg (0.177 mol%), T = 120 °C, reaction time = 6 h.

^a Batch operation with initial pressure of CO₂ = 1.17 MPa.

^b Semi-batch operation with constant pressure of CO₂ = 1.17 MPa.

anion of the functional group is known to activate the ring opening of AGE [2,3,11].

The reaction time has a prominent influence on the catalytic activity as revealed in Fig. 6 for the synthesis of AGC at semi-batch operation. The conversion of AGE in the first hour was 46% procuring a maximum of >98% in 6 h and thereafter remained nearly unchanged. The selectivity to AGC was very high and maintained throughout whole the reaction time. Thus, 6 h was chosen as reaction time for the further kinetic studies. In order to check a

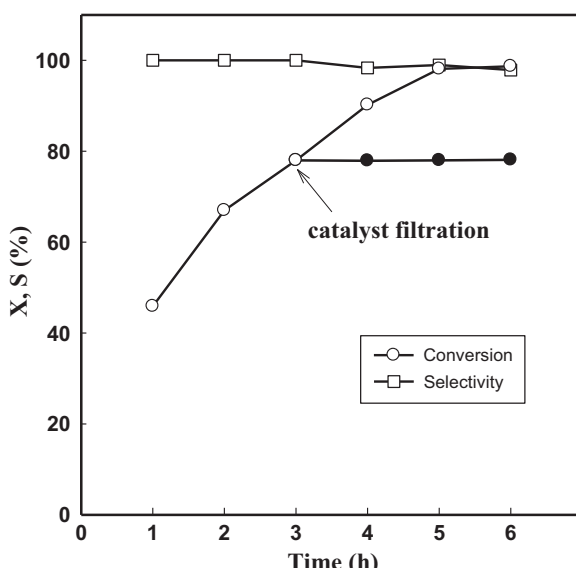


Fig. 6. Time variant AGE conversion and selectivity of AGC for F-ZIF-90 under semi-batch operation (AGE = 18.1 mmol, catalyst = 20 mg, T = 120 °C, reaction time = 6 h, P_{CO₂} = 1.17 MPa).

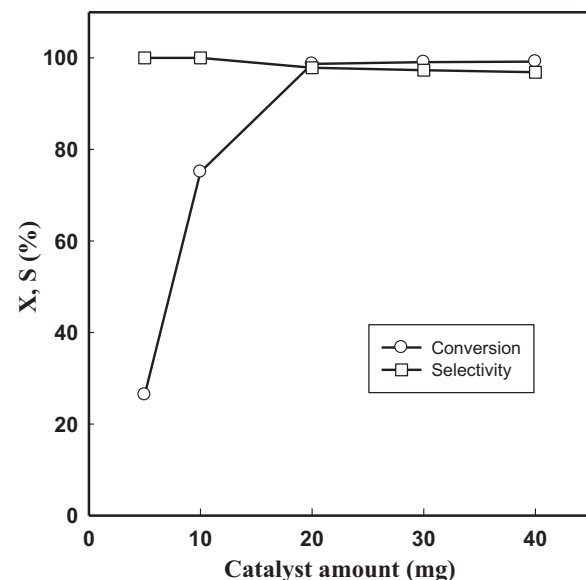


Fig. 7. Effect of catalyst amount on the reactivity of F-ZIF-90 under semi-batch operation. (AGE = 18.1 mmol, T = 120 °C, P_{CO₂} = 1.17 MPa, reaction time = 6 h).

Table 3

The effects of reaction temperature on the reactivity of F-ZIF-90.

Temp. (°C)	Conv. (%)	Sel. (%)	Yield (%)
60	4.1	85.4	3.5
80	37.1	93.1	34.5
100	62.2	96.8	60.2
120	98.7	97.9	96.6
140	99.4	96.2	95.6
160	99.2	90.8	90.1

Reaction conditions: AGE = 18.1 mmol, catalyst = 20 mg (0.177 mol%), reaction time = 6 h, P_{CO₂} = 1.17 MPa, semi-batch operation.

possible contribution of a homogeneous catalytic action of active zinc species leached into solution, hot catalyst filtration test was performed after 3 h of reaction. As shown in Fig. 6, no further AGE conversion in the filtrate occurred after catalyst removal at the reaction temperature, indicating that catalysis is not due to the soluble homogeneous species [35].

The effects of catalyst amount on the reactivity of F-ZIF-90 for the cycloaddition of CO₂ and AGE were studied under semi-batch operation at 120 °C with CO₂ pressure of 1.17 MPa and the results are shown in Fig. 7. Catalyst amounts varying from 5 to 40 mg which proportionately corresponds to 0.24 wt% (relative to AGE) to 1.9 wt% were investigated. The catalytic activity was found to be increasing with increase in the catalyst amount from 5 mg (0.24 wt%) to 20 mg (0.95 wt%) resulting from the increase in number of active sites available. Thereafter the increase in the catalyst amount does not show significant increase in the AGE conversion suggesting that 0.95 wt% is adequate enough of F-ZIF-90 effective for cycloaddition of AGE with CO₂.

The effects of reaction temperature on the synthesis of AGC were studied using F-ZIF-90 catalyst at the semi-batch operation, and the results are shown in Table 3. The conversion of AGE and the selectivity to AGC increased as the temperature increased from 60 °C to 120 °C. However, over 140 °C, the conversion remained nearly constant and the selectivity decreased. Therefore, all the following experiments were carried out at 120 °C. The main reaction byproduct was 3-allyloxy-1,2-propanediol.

The effects of CO₂ pressure on the reactivity of F-ZIF-90 at 120 °C after 6 h of reaction in the semi-batch reactor are shown in Table 4. The conversion of AGE increased as the CO₂ pressure increased

Table 4

The effects of CO₂ pressure on the reactivity of F-ZIF-90.

P _{CO₂} (MPa)	Conv. (%)	Sel. (%)	Yield (%)
0.35	91.1	94.8	86.3
0.90	95.1	95.3	90.6
1.05	96.0	97.5	93.6
1.17	98.7	97.9	96.6
1.30	97.6	98.2	95.8
1.50	95.1	98.7	93.9

Reaction conditions: AGE = 18.1 mmol, catalyst = 20 mg (0.177 mol%), T = 120 °C, reaction time = 6 h, semi-batch operation.

from 0.35 to 1.17 MPa. As CO₂ is one of the reactant, the conversion increased with higher concentration of CO₂ resulted at higher pressures. High CO₂ pressure could enhance the absorption of CO₂ in the solution of AGE. Zhang et al. [36] have reported an increase in the solubility of CO₂ in BMIMPF₆ by increasing CO₂ pressure. It has also been reported that high CO₂ pressure increases the turnover rate of the CO₂/cyclohexene oxide coupling reaction catalyzed by chromium salen complexes [16]. However, a decrease in the AGE conversion and AGC selectivity was observed when the CO₂ pressure increased from 1.17 to 1.5 MPa. A similar pressure-dependence trend has been observed in other catalytic systems [37–40]. Sun et al. [40] suggested that the initial increase in yield at low CO₂ pressure was due to an increase in the CO₂ concentration in the liquid phase of the reaction system, but too high pressure would reduce epoxide conversion because of lowered epoxide concentration in the vicinity of the catalyst or the worse mixing of the reactants by phase separation. Sun et al. [41] reported the two phases, a CO₂-rich gas phase and a liquid phase including epoxide, wherein CO₂ is also soluble. The selectivity to AGC increased continuously when the CO₂ pressure increased from 0.35 to 1.5 MPa, since high CO₂ pressure may inhibit the formation of byproducts or the backward decomposition of AGC to AGE and CO₂.

Various epoxide substrates were subjected to the cycloaddition reaction using F-ZIF-90 under the optimized conditions determined as explained above. The results are summarized in Table 5. All the epoxides tested gave high conversions, with the exception of cyclohexene oxide, which might be due to the high steric hindrance caused by cyclohexene ring [42]. It was also observed that the epoxide substrates with an additional ether oxygen linkage in the side chain (AGE and phenyl glycidyl ether), had higher catalytic activity compared to other epoxide substrates. This extra edge in activity is witnessed in many works concerned with epoxide–CO₂ cycloaddition reactions [10,43–47]. Our previous work [47], attributed this high activity to the interaction of ether oxygen and COOH group

Table 5

The reactivity of F-ZIF-90 for various epoxides.

Catalyst	Conv. (%)	Sel. (%)	Yield (%)
Styrene oxide	62.8	99.3	62.4
Propylene oxide	89.0	98.6	87.8
Epichlorohydrin	95.2	99.1	94.3
Phenyl glycidyl ether	96.7	98.7	96.3
Cyclohexene oxide	2.4	98.0	2.4

Reaction conditions: epoxide = 18.1 mmol, F-ZIF-90 = 20 mg (0.177 mol%), T = 120 °C, reaction time = 6 h, P_{CO₂} = 1.17 MPa, semi-batch operation.

of the quaternized glycine catalyst after DFT studies. The role of F-ZIF-90 with the ether oxygen needs more detailed studies.

We compared the catalytic performance of the F-ZIF-90 with other MOF-based heterogeneous catalysts reported in the literature (Table 6). All the catalysts operated at relatively mild reaction conditions (temperature 80–150 °C and CO₂ pressure 0.7–2.02 MPa) without using any co-catalyst and solvent except Co-MOF-74 which used chlorobenzene as a solvent. The F-ZIF-90 exhibited the TON superior to the best yields achieved so far by the different MOFs [28,35,48–53].

Considering the above results and previous works [16,54–59] we attempted to propose plausible mechanism (Scheme 2) including the probable sequence of events occurred in the F-ZIF-90 catalyzed cycloaddition of CO₂ with AGE, yielding AGC. The AGE molecules approach the zinc metal atom, forming a metal–oxygen bonding with the epoxide ring, then nucleophilic anion (iodide ion) on F-ZIF-90 is able to initiate an attack on the least hindered (β) carbon atom of the epoxide ring. Ring opening of the epoxide occurs, followed by formation of a new C–I covalent bond. The ring-opened epoxide moiety engages in attack with carbon dioxide, yielding an alkyl carbonate anionic species, which eventually yields AGC upon subsequent ring closure and catalyst regeneration.

Regarding the reusability of F-ZIF-90, the catalytic activity of the recycled catalyst was evaluated at 120 °C under constant CO₂ pressure of 1.17 MPa for 6 h. In the recycle experiment, the used catalyst was filtered, washed with acetone, and air dried before use. Fig S1 in the Supplementary information shows the XRD results of reused catalyst and it confirmed the maintenance of its original structure of F-ZIF-90 after use. However, the yield of AGC decreased from 96.6% (fresh) to 58.3% (recycled). The BET surface area decreased from 763 to 548 m²/g after reuse. Miralda et al. [28] observed similar trends, that is, decrease in both BET surface area and catalytic activity as well as loss of the structural features upon further reuse of ZIF-8 in the cycloaddition of CO₂ to epichlorohydrin. They suggested that a synergistic effect of the high pressure of CO₂ and the

Table 6

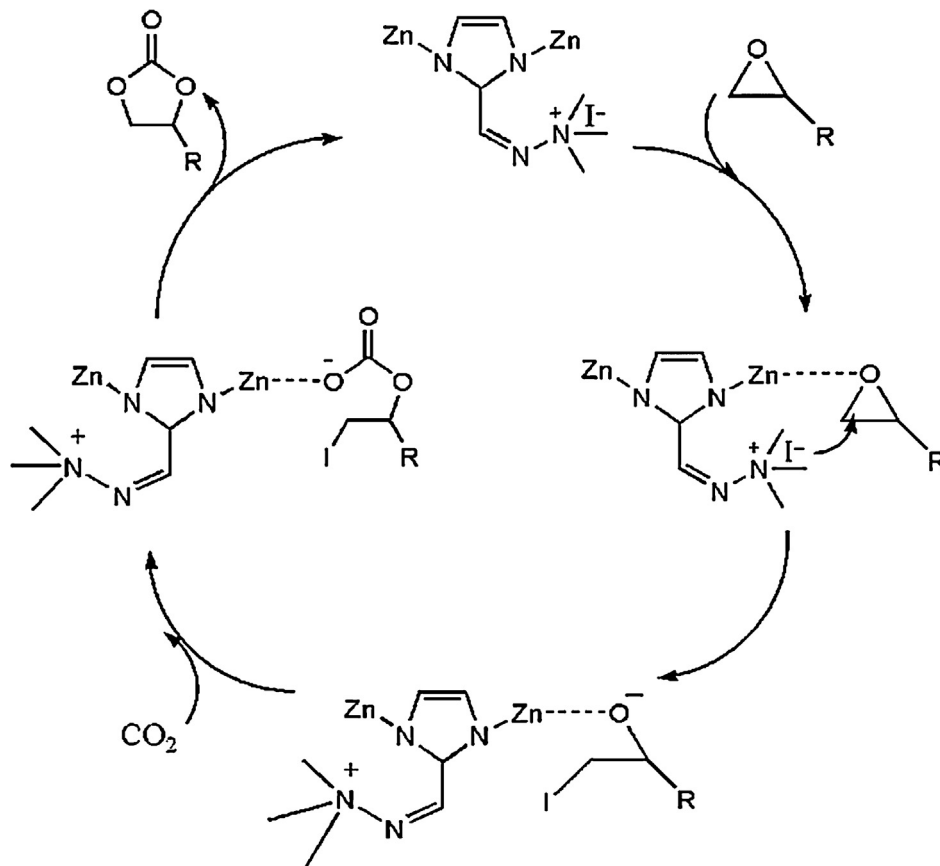
Comparison of F-ZIF-90 with other MOF-based catalysts in the cycloaddition of CO₂ and epoxides.

MOF	Epoxide	Cat. amount ^a (mol%)	T (°C)	P _{CO₂} (MPa)	Time (h)	Yield (%)	TON ^b	Ref.
Mg-MOF-74	SO	1.88	100	2	1	50	27	[48]
ZIF-8	EPCH	0.44	100	0.7	4	32.8	75	[28]
ZIF-8-f	EPCH	0.44	100	0.7	4	49.1	112	[28]
ZIF-8	SO	0.7	100	0.74	5	55	79	[49]
UIO-66-NH ₂	SO	2.1	100	2	1	58	28	[50]
MIL-68(IndNH ₂)	SO	9.1	150	0.8	8	74	8	[51]
Cr-MIL-101	SO	1.2	80	0.8	14	62	52	[34]
Co-MOF-74	SO ^c	1.6	100	2.02	4	96	60	[52]
IRMOF-1	AGE	0.59	120	1.2	6	20.1	34	[38]
IRMOF-3	AGE	0.55	120	1.2	6	44.1	80	[38]
F-IRMOF-3(Bul)	AGE	0.43	120	1.2	6	92.3	215	[38]
ZnHipBipy-B	AGE	1.6	120	1.2	6	40.7	25	[53]
ZIF-90	AGE	0.430	120	1.17	6	43.4	101	This work
F-ZIF-90	AGE	0.177	120	1.17	6	96.6	547	This work
F-ZIF-90	AGE	0.088	120	1.17	6	75.1	855	This work

^a [(Moles of metal atom)/(moles of epoxide)] × 100 (%).

^b TON = moles of cyclic carbonate formed/moles of metal in MOF catalyst.

^c Chlorobenzene was used as a solvent.



Scheme 2. Proposed mechanism for the cycloaddition of CO_2 and epoxide with F-ZIF-90.

high temperature along with blocking of the active sites by carbonaceous products could be the reason of the activity loss and crystalline instability of ZIF-8 after the reuse.

4. Conclusion

Quaternary ammonium group functionalized F-ZIF-90 was successfully prepared through the reaction of ZIF-90 with hydrazine followed by the quaternization by alkyl halide. In the synthesis of the cyclic carbonate from AGE and carbon dioxide, the F-ZIF-90 showed excellent catalytic activity without the use of any solvent and co-catalyst. The AGE yield showed maxima as the temperature and CO_2 pressure increased. However, the loss of its superior catalytic performance and distinctive crystalline nature was inevitable when it was reused.

Acknowledgements

This study was supported by the National Research Foundation of Korea (2012-001507), Global Frontier Program, BK21 PLUS, and KBSI.

Appendix A. Supplementary data

Supplementary data associated with this article can be found, in the online version, at <http://dx.doi.org/10.1016/j.cattod.2014.05.022>.

References

- [1] S. Klaus, M.W. Lehenmeier, C.E. Anderson, B. Rieger, *Coord. Chem. Rev.* 255 (2011) 1460–1479.
- [2] M. North, R. Pasquale, C. Young, *Green Chem.* 12 (2010) 1514–1539.
- [3] J. Melendez, M. North, P. Villuendas, *Chem. Commun.* (18) (2009) 2577–2579.
- [4] M. Aresta, A. Dibenedetto, *Dalton Trans.* (28) (2007) 2975–2992.
- [5] S. Zhang, Y. Chen, F. Li, X. Lu, W. Dai, R. Mori, *Catal. Today* 115 (2006) 61–69.
- [6] S. Inoue, N. Yamazaki, *Organic and Bioorganic Chemistry of Carbon Dioxide*, Kodansha Ltd., Tokyo, 1981.
- [7] E.H. Lee, J.Y. Ahn, M.D. Manju, D.W. Park, S.W. Park, I. Kim, *Catal. Today* 131 (2008) 130–134.
- [8] D.J. Daresbourg, R.M. Mackiewicz, A.L. Phelps, D.R. Billodeaux, *Acc. Chem. Res.* 37 (2004) 836–844.
- [9] J. Tharun, D.W. Kim, R. Roshan, Y.S. Hwang, D.W. Park, *Catal. Commun.* 31 (2013) 62–65.
- [10] K.R. Roshan, G. Mathai, J. Kim, J. Tharun, G.A. Park, D.W. Park, *Green Chem.* 14 (2012) 2933–2940.
- [11] G.W. Coates, D.R. Moore, *Angew. Chem. Int. Ed.* 43 (2004) 6618–6639.
- [12] J.J. Peng, Y. Deng, *New J. Chem.* 25 (2001) 639–641.
- [13] H. Yasuda, L. He, T. Sakakura, C. Hu, *J. Catal.* 233 (2005) 119–122.
- [14] J. Tharun, D.W. Kim, R. Roshan, A.C. Kathalikkattil, M. Selvaraj, D.W. Park, *RSC Adv.* 3 (2013) 14290–14293.
- [15] J. Tharun, M.M. Dharmam, Y. Hwang, R. Roshan, M.S. Park, D.W. Park, *Appl. Catal., A: Gen.* 419 (2012) 178–184.
- [16] F. Castro-Gomez, G. Salassa, A.W. Kleij, C. Bo, *Chem. Eur. J.* 19 (2013) 6289–6298.
- [17] Z. Wang, S.M. Cohen, J. Am. Chem. Soc. 129 (2007) 12368–12369.
- [18] S. Natarajan, S. Mandal, *Angew. Chem. Int. Ed.* 47 (2008) 4798–4828.
- [19] H. Li, M. Eddaoudi, M. O’Keeffe, O.M. Yaghi, *Nature* 402 (1999) 276–279.
- [20] M. O’Keeffe, M. O’Keeffe, N.W. Ockwig, H.K. Chae, M. Eddaoudi, J. Kim, *Nature* 423 (2003) 705–714.
- [21] R.E. Morris, P.S. Wheatley, *Angew. Chem. Int. Ed.* 47 (2008) 4966–4981.
- [22] B. Chen, C. Liang, J. Yang, D.S. Contreras, Y.L. Clancy, E.B. Lobkovsky, O.M. Yaghi, S. Dai, *Angew. Chem. Int. Ed.* 45 (2006) 1390–1393.
- [23] O. Kahn, *Acc. Chem. Res.* 33 (2000) 647–657.
- [24] J. Gascon, U. Aktay, M.D. Hernandez-Alonso, G.P.M. van Klink, F. Kapteijn, *J. Catal.* 261 (2009) 75–87.
- [25] F.X. Llabres i Xamena, F.G. Cirujano, A. Corma, *Microporous Mesoporous Mater.* 157 (2012) 112–117.
- [26] A. Phan, C.J. Doonan, F.J. Uribe-Romo, C.B. Knobler, M. O’Keeffe, O.M. Yaghi, *Acc. Chem. Res.* 43 (2010) 58–67.
- [27] R. Banerjee, A. Phan, B. Wang, C.B. Knobler, H. Furukawa, M. O’Keeffe, O.M. Yaghi, *Science* 319 (2008) 939–943.
- [28] C.M. Miralda, E.E. Macias, M. Zhu, P. Ratnasamy, M.A. Carreon, *ACS Catal.* 2 (2012) 180–183.

- [29] W. Morris, C.J. Doonan, H. Furukawa, R. Banerjee, O.M. Yaghi, *J. Am. Chem. Soc.* 130 (2008) 12626–12627.
- [30] T. Yang, T.S. Chung, *J. Mater. Chem., A: Mater. Energy Sustainability* 1 (2013) 6081–6090.
- [31] F.K. Shieh, S.C. Wang, S.Y. Leo, K.C.W. Wu, *Chem. Eur. J.* DOI: 10.1002/chem.201301560.
- [32] A. Huang, J. Caro, *Angew. Chem. Int. Ed.* 50 (2011) 4979–4982.
- [33] X.C. Huang, Y.Y. Lin, J.P. Zhang, X.M. Chen, *Angew. Chem. Int. Ed.* 45 (2006) 1557–1559.
- [34] Z.A. ALOthman, *Materials* 5 (2012) 2874–2902.
- [35] O.V. Zalomaeva, A.M. Chibiryav, K.A. Kovalenko, O.A. Kholdoeva, B.S. Balzhinimaev, V.P. Fedin, *J. Catal.* 298 (2013) 179–185.
- [36] S. Zhang, X. Yuan, Y. Chen, X. Zhang, *J. Chem. Eng. Data* 50 (2005) 1582–1585.
- [37] L.F. Xiao, F.W. Li, J.J. Peng, C.G. Xia, *J. Mol. Catal. A: Chem.* 253 (2006) 265–269.
- [38] Y.J. Kim, D.W. Park, *J. Nanosci. Nanotechnol.* 13 (2013) 2307–2312.
- [39] Y. Xie, Z.F. Zhang, T. Jiang, J.L. He, B.X. Han, T.B. Wu, K.L. Ding, *Angew. Chem. Int. Ed.* 46 (2007) 7255–7258.
- [40] J. Sun, W. Cheng, W. Fan, Y. Wang, Z. Meng, S. Zhang, *Catal. Today* 148 (2009) 361–367.
- [41] J. Sun, S. Fujita, F. Zhao, M. Arai, *Green Chem.* 6 (2004) 613–616.
- [42] C. Qi, J. Ye, W. Zeng, H. Jiang, *Adv. Synth. Catal.* 352 (2010) 1925–1933.
- [43] L.F. Xiao, F.W. Li, C.G. Xia, *Appl. Catal., A: Gen.* 279 (2005) 125–129.
- [44] F. Wu, X.Y. Dou, L.N. He, C.X. Miao, *Lett. Org. Chem.* 7 (2010) 73–78.
- [45] S.S. Wu, X.W. Zhang, W.L. Dai, S.F. Yin, W.S. Li, Y.Q. Ren, C.T. Au, *Appl. Catal., A: Gen.* 341 (2008) 106–111.
- [46] J.Q. Wang, D.L. Kong, J.Y. Chen, F. Cai, L.N. He, *J. Mol. Catal. A: Chem.* 249 (2006) 143–148.
- [47] J. Tharun, G. Mathai, R. Roshan, A.C. Kathalikkattil, B. Kim, D.W. Park, *Phys. Chem. Chem. Phys.* 15 (2013) 9029–9033.
- [48] D.A. Yang, H.Y. Cho, J. Kim, S.T. Yang, W.S. Ahn, *Energy Environ. Sci.* 5 (2012) 6465–6473.
- [49] M. Zhu, D. Srinivas, S. Bhogeswararao, P. Ratnsamy, M.A. Carreon, *Catal. Commun.* 32 (2013) 36–40.
- [50] J. Kim, S.N. Kim, H.G. Jang, G. Seo, W.S. Ahn, *Appl. Catal., A: Gen.* 453 (2013) 175–180.
- [51] T. Lescouet, C. Chizallet, D. Farrusseng, *ChemCatChem* 2 (2012) 1725–1728.
- [52] H.Y. Cho, D.A. Yang, J. Kim, S.Y. Jeong, W.S. Ahn, *Catal. Today* 185 (2012) 35–40.
- [53] A.C. Kathalikkattil, D.W. Park, *J. Nanosci. Nanotechnol.* 13 (2013) 2230–2235.
- [54] D.W. Kim, R. Roshan, J. Tharun, A.C. Kathalikkattil, D.W. Park, *Korean J. Chem. Eng.* 30 (2013) 1973–1984.
- [55] C. Aprile, F. Giacalone, P. Agricento, L.F. Liotta, J.A. Martens, P.P. Pescarmona, M. Gruttaduria, *ChemSusChem* 4 (2011) 1830–1837.
- [56] S. Liang, H. Liu, T. Jiang, J. Song, G. Yang, B. Han, *Chem. Commun.* 47 (2011) 2131–2133.
- [57] J. Ma, J. Liu, Z. Zhang, B. Han, *Green Chem.* 14 (2012) 2410–2420.
- [58] K.R. Roshith, T. Jose, A.C. Kathalikkattil, D.W. Kim, B. Kim, D.W. Park, *Appl. Catal., A: Gen.* 467 (2013) 17–25.
- [59] J.Q. Wang, K. Dong, W.G. Cheng, J. Sun, S.J. Zhang, *Catal. Sci. Technol.* 2 (2012) 1480–1484.